Accelerated DNA methylation age: Associations with PTSD and neural integrity

Erika J. Wolf [a,b,*], Mark W. Logue [c,d,e], Jasmeet P. Hayes [a,b,g], Naomi Sadeh [a,b], Steven A. Schichman [f], Annjanette Stone [f], David H. Salat [g], William Milberg [h,i], Regina McGlinchey [h,i], Mark W. Miller [a,b]

[a] National Center for PTSD, Behavioral Science Division, VA Boston Healthcare System, Boston, MA, USA
[b] Department of Psychiatry, Boston University School of Medicine, Boston, MA, USA
[c] Research Service, VA Boston Healthcare System, Boston, MA, USA
[d] Biomedical Genetics, Boston University School of Medicine, Boston, MA, USA
[e] Department of Biostatistics, Boston University School of Public Health, Boston, MA, USA
[f] Pharmacogenomics Analysis Laboratory, Research Service, Central Arkansas Veterans Healthcare System, Little Rock, AR, USA
[g] Neuroimaging Research for Veterans Center, VA Boston Healthcare System, Boston, MA, USA
[h] Geriatric Research Educational and Clinical Center and Translational Research, Center for TBI and Stress Disorders, VA Boston Healthcare System, Boston, MA, USA
[i] Department of Psychiatry, Harvard Medical School, Boston, MA, USA

ARTICLE INFO

ABSTRACT

Background: Accumulating evidence suggests that posttraumatic stress disorder (PTSD) may accelerate cellular aging and lead to premature morbidity and neurocognitive decline.
Methods: This study evaluated associations between PTSD and DNA methylation (DNAm) age using recently developed algorithms of cellular age by Horvath (2013) and Hannum et al. (2013). These estimates reflect accelerated aging when they exceed chronological age. We also examined if accelerated cellular age manifested in degraded neural integrity, indexed via diffusion tensor imaging.
Results: Among 281 male and female veterans of the conflicts in Iraq and Afghanistan, DNAm age was strongly related to chronological age ($rs \sim .88$). Lifetime PTSD severity was associated with Hannum DNAm age estimates residualized for chronological age ($\beta = .13$, $p = .032$). Advanced DNAm age was associated with reduced integrity in the genu of the corpus callosum ($\beta = -.17$, $p = .009$) and indirectly linked to poorer working memory performance via this region (indirect $\beta = -.05$, $p = .029$). Horvath DNAm age estimates were not associated with PTSD or neural integrity.
Conclusions: Results provide novel support for PTSD-related accelerated aging in DNAm and extend the evidence base of known DNAm age correlates to the domains of neural integrity and cognition.

Published by Elsevier Ltd.

1. Introduction

Chronic psychological stress may accelerate cellular aging and lead to early onset of age-related disease, neurodegeneration, and pre-mature mortality (Epel, 2009; Epel et al., 2004; Lindqvist et al., 2015). Posttraumatic stress disorder (PTSD) has been identified as a chronic stress-related condition that may accelerate cellular aging, increasing risk for neuronal cell death via oxidative stress, inflammatory, and other pathophysiological pathways (Lohr et al., 2015; Miller and Sadeh, 2014; Moreno-Villanueva et al., 2013; Williamson et al., 2015). Repeated activation of the hypothalamic–pituitary–adrenal (HPA) axis system, chronic sleep deprivation, and other PTSD-related disturbances are hypothesized to increase reactive oxygen species and decrease the capacity of antioxidants to protect neurons from the toxic effects of oxidative stress (Miller and Sadeh, 2014). Chronic PTSD may also lead to glucocorticoid-mediated increases in peripheral and central nervous system inflammation, and dysregulated autonomic and metabolic processes (Epel, 2009; Lohr et al., 2015; Williamson et al., 2015) thereby degrading cellular integrity and ultimately leading to cell death.

* Corresponding author at: National Center for PTSD (116B-2), VA Healthcare System, 150 South Huntington Ave., Boston, MA, USA.
E-mail address: erika.wolf@va.gov (E.J. Wolf).

Within the past two years, important advances have been made in the use of DNA methylation (DNAm) data to index chronological age. Hannum et al. (2013) developed a model of cellular age (DNAm age) based on methylation levels measured in whole blood at 71 DNA loci and found this metric of DNAm age to be highly correlated with chronological age ($r = .96$). The majority of the loci in this algorithm were located in or near genes important for the development of age-related disease, DNA damage and repair, and/or oxidative stress (Hannum et al., 2013). In the same year, Horvath (2013) independently developed a multi-tissue DNAm age algorithm using 353 loci and found this metric to also correlate highly with chronological age at $r = .96$. Despite these impressive associations, the biological mechanism(s) linking epigenetic variation to chronological age remain unclear.

Preliminary cross-sectional evidence suggests that exposure to pathogenic environmental factors may influence DNAm age, yielding higher estimates than would be expected based on chronological age. For example, Horvath et al. (2014) showed that obesity was associated with accelerated DNAm age in human liver tissue. Accelerated DNAm age relative to chronological age has also been linked to indices of disease, including cross-sectional associations with worse performance on measures of fluid intelligence, grip strength, and lung function (Marioni et al., 2015b). Likewise, a meta-analysis of over 4600 older-aged adults found that for every five year-increase in DNAm age relative to chronological age using the Hannum et al. (2013) and Horvath (2013) algorithms, there were 21% and 11% increases, respectively, in all-cause mortality (Marioni et al., 2015a).

To our knowledge, only one published study (Boks et al., 2015) has examined associations between trauma and/or PTSD and DNAm age. In that study of 96 male soldiers, trauma exposure was positively related to DNAm age per the Horvath (2013) algorithm, while self-reported PTSD symptoms unexpectedly predicted decreased DNAm age estimates over the course of approximately one year (Boks et al., 2015). However, chronological age was not included in this analysis so it remains unclear how these findings relate to discrepancies between DNAm age and chronological age. In this study, we aimed to address this limitation by examining the association between the cumulative lifetime burden of PTSD and DNAm age, controlling for chronological age.

We also tested the hypothesis that accelerated DNAm age is correlated with indices of neural integrity in regions known to degrade with normal aging. Gray matter volume and cortical thickness decrease globally with advancing age (Good et al., 2001; Resnick et al., 2003) with these effects most evident in prefrontal regions (Resnick et al., 2003; Salat et al., 2004, 2005b). Studies of white matter microstructural integrity (i.e., diffusion tensor imaging; DTI) have found the most consistent effects using measures of fractional anisotropy (FA) in the prefrontal cortex (Bennett et al., 2010; Burgmans et al., 2010; Pfefferbaum et al., 2000; Salat et al., 2005a) and the genu of the corpus callosum (Bennett et al., 2010; Burgmans et al., 2010; Kochunov et al., 2012; Pfefferbaum et al., 2000; Salat et al., 2005a; Voineskos et al., 2012; Zahr et al., 2009), which connects the right and left prefrontal cortices (Hofer and Frahm, 2006). These regions are involved in higher-order executive functions, such as working memory and response inhibition (Zahr et al., 2009), which also show age-related declines (Park et al., 2002). Based on this, a final aim of this study was to examine possible links between accelerated DNAm age and performance on executive function tasks that depend on these regions of interest (ROIs).

We hypothesized that lifetime PTSD severity (as indexed by a latent variable capturing PTSD severity across three time intervals), would be associated with accelerated DNAm age estimates relative to chronological age. We also expected that advanced DNAm age would be negatively related to microstructural integrity (FA values)

in areas of the brain previously linked to age-related degeneration (the frontal cortex and genu) and to performance on executive function tasks mediated by our ROIs.

2. Materials and methods

2.1. Participants

Horvath (2013) and Hannum et al. (2013) DNAm age estimates were available for 289 veterans of the conflicts in Iraq and Afghanistan assessed at the Translational Research Center for TBI and Stress Disorders, a VA RR&D Traumatic Brain Injury Center of Excellence at VA Boston Healthcare System. Exclusion criteria included history of seizures (unrelated to head injury), neurological illness, current bipolar or psychotic disorder, severe depression or anxiety, active homicidal and/or suicidal ideation with intent, cognitive disorder due to general medical condition other than traumatic brain injury (TBI), and unstable psychological diagnosis that interfered with accurate data collection. For the MRI portion of the assessment, additional exclusionary criteria included pregnancy and having a metal implant, shrapnel, aneurysm clip, or pacemaker. Eight participants were excluded from these analyses due to history of moderate or severe traumatic brain injury, yielding a total sample size of 281 for analyses focused on PTSD and DNAm age. Of these, DTI data were available for 241 participants.

Of the 281 veterans with DNAm age data, the mean age was 31.93 years (SD: 8.40, range: 19–58) and 87.9% were male ($n = 247$). Self-reported race and ethnicity was as follows: 70.5% white, 15.3% Hispanic or Latino/a, 8.5% black or African American, 2.1% Asian, 1.1% American Indian (2.5% did not self-report). 55.9% and 74.0% of the sample met DSM-IV-TR diagnostic criteria for current and lifetime PTSD, respectively, per the Clinician Administered PTSD Scale (CAPS; Blake et al., 1995), as defined by the DSM-IV-TR algorithm with clinician frequency ratings ≥ 1 and severity ratings ≥ 2 required for endorsement of the criterion (along with the distress/impairment criteria; Weathers et al., 1999). The mean post-deployment CAPS score was 63.08 (SD = 34.63).

2.2. Procedures

Veterans gave informed consent and then provided fasting blood samples, underwent diagnostic interviewing by a PhD-level clinician, completed a neuropsychological battery, and underwent MRI acquisition. Psychiatric diagnoses were confirmed by an expert consensus team. The protocol was reviewed by the appropriate institutional review boards.

2.2.1. DNA genotyping and methylation

Peripheral whole blood samples were obtained and DNA extracted from buffy coat. Genotyping, relevant here for capturing DNA ancestral variation via principal components (PC) analysis (see Supplementary Methods), was conducted on the hybridized DNA samples using the Illumina Human Omni 2.5–8 microarray and scanned with an Illumina iScan System (Illumina, San Diego, CA). For DNAm quantification, hybridized bisulfite-modified DNA (achieved via Zymo EZ-96 DNA Methylation Kits D5004) were whole-genome amplified, fragmented, precipitated, resuspended, and hybridized to Illumina HumanMethylation 450k beadchips and then scanned with an Illumina iScan System (Illumina, San Diego, CA). The Horvath age estimate was computed using an R script supplied by Dr. Horvath (http://labs.genetics.ucla.edu/horvath/dnamage/). As this script includes a normalization step, non-normalized average beta values as exported from Genomestudio were used as input after removing two subjects with low intensity scores. The Hannum et al. DNAm age estimates were computed in R directly using a linear function of the 89

covariates of the "all data" model as reported by Hannum et al. (2013). This method was run on data post-normalization (normalized via the beta mixture quantile dilation method; Teschendorff et al., 2013) and imputation of sporadic missing values using a K nearest-neighbor method as implemented in the Bioconductor impute package (http://www.bioconductor.org/packages/release/bioc/html/impute.html; see Supplementary Materials for additional details). Of the 89 probes in the model, two were dropped during the quality control process (cg25428494 and ch.13.39564907R) and therefore the Hannum DNAm age estimates are based on observed methylation at 87 probes. As differential white blood cell (WBC) count estimates were not available for the data, the proportion of WBCs (CD8 cells, CD4 cells, NK cells, B cells, monocytes, granulocytes, and lymphocytes) were estimated from the methylation directly using the Houseman method (Houseman et al., 2012; Jaffe and Irizarry, 2014) as implemented in the Bioconductor minfi package (Aryee et al., 2014). Additional details are provided in the Supplementary Materials.

2.2.2. MRI/DTI acquisition and processing

Structural imaging data were acquired on a 3-Tesla Siemens TIM TRIO whole-body MRI scanner. Two T1-weighted anatomical scans (voxel size = 1 mm^3, TR = 2530 ms, TE = 3.32 ms, FOV = 256 × 256, # of slices = 176) were acquired and averaged to create a single high contrast-to-noise image. DTI acquisition involved one acquisition of 60 directions, FOV = 256, Matrix = 128 × 128, TR = 10,000 ms, TE = 103 ms, 2 × 2 × 2 mm voxels, b value = 700 s/mm^2. We used FreeSurfer image analysis suite (http://surfer.nmr.mgh.harvard.edu/) and The Oxford Center for Functional Magnetic Resonance Imaging of the Brain (FMRIB) FSL software package (http://www.fmrib.ox.ac.uk/fsl/) for data analysis. Images were corrected for motion and eddy currents using FreeSurfer. Additional DTI processing details, including a list of the frontal parcellations evaluated, are provided in the Supplementary Materials.

2.3. Measures

PTSD diagnosis and symptom severity was assessed with the Clinician Administered PTSD Scale for DSM-IV (Blake et al., 1995), the gold-standard structured diagnostic interview for PTSD assessment. PTSD symptom severity was assessed for three periods of time: past-month (i.e., current PTSD), pre-deployment (if relevant pre-military trauma), and post-deployment (worst 30-day period of symptoms following deployment). We used factor analyses to combine these three severity measurements and develop a metric of PTSD severity across the lifetime (see below). Participants were also administered a comprehensive neuropsychological battery by a psychologist. From this, we selected seven subtests from three tests (see Supplementary Methods) for use as an index of working memory. The measures included were: Digit Span Forward and Backward (Wechsler, 1997); Color–Word Interference Test (a Stroop-type task; Delis et al., 2001); and Letter/Number Sequencing from the Trail Making Test (Delis et al., 2001).

2.4. Data analyses

Following Marioni et al. (2015b) and Horvath et al. (2014), we first conducted regressions in which the Hannum or Horvath DNAm age estimates were regressed on self-reported chronological age in separate analyses and we saved the unstandardized residuals (hereafter "DNAm age residuals") from these equations as a new variable for use in our main analyses. Positive residuals indicate accelerated aging (i.e., estimated age was over-predicted relative to chronological age). We next used confirmatory factor analysis (CFA) to develop a metric of the lifetime severity of PTSD symptoms by specifying pre-military, post-military, and current PTSD

symptom severity scores as indicators of latent lifetime PTSD severity and saved factor scores (reflecting each individual's level of PTSD symptoms across the lifespan) for use in subsequent analyses. Study hypotheses were then tested using a series of regression models. The first evaluated lifetime PTSD severity as a predictor of the Hannum DNAm age residuals, controlling for sex, the top two genetic PCs (reflecting ancestry), and WBCs; the Horvath DNAm age residuals were examined in a second identical model. We then evaluated the association between DNAm age residuals and FA values in our ROIs, with separate models for each class of related ROIs (i.e., one model for right frontal cortex, one for left frontal cortex, and a model for the genu of the corpus callosum). Age and sex were included as covariates of the DTI parameters, and sex, the two PCs, and WBCs were included as covariates of the DNAm age residuals. We also tested if DNAm age residuals were associated with working memory performance via our ROIs in a subsequent path model (using confirmatory factor analysis to form a latent working memory variable). All models were computed using a robust maximum likelihood estimator (a "sandwich" estimator which adjusts the standard errors to protect against Type I error) in Mplus 7.11 (Muthén and Muthén, 2012) and all paths in the model were estimated simultaneously. For models with more than one dependent variable (i.e., the frontal cortex parcellations), the residual correlations among the dependent variables were estimated. The fit of the models was evaluated using standard fit indices and guidelines (Hu and Bentler, 1999; see Supplementary Materials). Standardized regression coefficients are reported throughout the manuscript text.

3. Results

3.1. DNAm age associations with chronological age

The Hannum DNAm age estimates were highly correlated with self-reported chronological age (r = .88, p < .001) and the Horvath DNAm age algorithm yielded a virtually identical estimate (r = .87, p < .001). The two DNAm age estimates correlated with each other at r = .88, p < .001, but the residual variables (with chronological age regressed out) were only moderately associated with each other (r = .49, p < .001). Neither the Hannum nor Horvath DNAm age residuals were associated with chronological age (rs = .002 and .001, respectively, both ps > .97). Hannum DNAm age unstandardized residuals ranged from −11.82 to 19.24 years (M = .05, SD = 4.25) while Horvath DNAm age unstandardized residuals ranged from −13.04 to 16.90 years (M = .03, SD = 3.81).

3.2. Latent lifetime PTSD severity and accelerated aging

The CFA of latent lifetime PTSD severity revealed that post-military symptoms loaded most strongly on the lifetime factor (β = .90, p < .001), followed by current symptoms (β = .85, p < .001), and pre-military symptoms (β = .22, p = .004). Lifetime PTSD severity factor scores were positively associated with the Hannum DNAm age residuals (β = .13, p = .032), controlling for covariates.[1,2]

---

[1] We also evaluated if PTSD symptom burden might be associated with Hannum DNAm age residuals by creating a variable that reflected PTSD symptom severity multiplied by the duration of those symptoms (in months). We did this only for the post-military time period because of concerns related to outliers in the pre-military duration variable and because we did not expect current symptom duration to have sufficient chronicity to accelerate aging. Data on post-military PTSD burden were available for 166 participants. Post-military PTSD burden was positively associated with Hannum DNAm age residuals (β = .12, p = .026), controlling for the same covariates as in our main analysis.

[2] We also evaluated if the effects of PTSD on DNAm age residuals were moderated by sex and found no significant interaction effect.

Table 1
Fit of primary regression/structural models.

Model	X^2 (df)	RMSEA	SRMR	CFI	TLI
Lifetime PTSD factor (measurement model)[a]	0[**] (0)	0	0	1.0	1.0
PTSD → DNAm Res (Hannum & Horvath)[a]	0[**] (0)	0	0	1.0	1.0
DNAm Res → right frontal (FA)	97.54[*] (71)	.039	.044	.980	.957
DNAm Res → left frontal (FA)	87.24 (71)	.031	.038	.986	.969
DNAm Res → genu (FA)	8.97 (8)	.022	.021	.976	.943
DNAm Res → genu (RD)	9.52 (8)	.028	.022	.957	.90
DNAm Res → genu (ADC)	10.75 (8)	.038	.023	.888	.733
DNAm Res → genu (AxD)	6.32 (8)	<.001	.017	1.00	1.25
Working memory factor (measurement model)	7.63 (7)	.020	.023	.998	.993
DNAm Res → genu (FA) → working memory	121.60[*] (89)	.041	.053	.928	.905

Note: All models involving brain regions included the Hannum et al. DNAm age residuals as the primary predictor (results for the Horvath model are listed in the Supplementary Materials). DNAm Res = DNA methylation residuals; RMSEA = root mean square error of approximation; SRMR = standardized root mean square residual; CFI = confirmatory fit index; TLI = Tucker–Lewis index; FA = fractional anisotropy; RD = radial diffusivity; ADC = apparent diffusion coefficient; AxD = axial diffusivity.

[a] These models are just identified (i.e., df = 0), thus they will always achieve perfect fit.

[*] $p < .05$.

[**] $p < .001$.

CD4 t-cell counts were also significantly associated with DNAm age residuals and in total, this model, with PTSD, sex, and cell counts included, explained 9% of the variance in Hannum DNAm age residuals (see Table 1 for the fit of all models, which was consistent with good fit for all analyses, Table 2 for coefficients, and Supplementary Fig. 1). Analyses examining the influence of potential confounders, including substance use, other mental health diagnoses, trauma exposure and traumatic brain injury, are reported in the Supplementary Materials. A parallel analysis revealed no significant association between lifetime PTSD severity factor scores and DNAm age residuals computed using the Horvath method ($\beta = .02$, $p = .819$; see Table 2). Based on this, we omitted Horvath DNAm age from subsequent consideration, though results pertaining to Horvath DNAm age and neural integrity are listed in Supplementary Tables 1 and 2 for the sake of completeness.

3.3. Accelerated aging and neural integrity

The analysis evaluating the association between the Hannum DNAm age residuals and FA in the right frontal cortex yielded no significant effects for DNAm age residuals (see Table 3). The model predicting FA in the left frontal cortex revealed two nominally significant DNAm age residual effects: DNAm age residuals were negatively associated with FA in the left rostral anterior cingulate cortex ($\beta = -.13$, $p = .016$) and with FA values in the left rostral middle frontal gyrus ($\beta = -.13$, $p = .046$). Neither of these associations survived correction for multiple testing within the model using a Bonferonni approach. Chronological age was associated with most frontal parcellations (see Table 3). In the third model, DNAm age residuals were negatively associated with FA in the genu ($\beta = -.17$,

$p = .009$; see Table 4) and the model explained 11% of the variance in this ROI. Based on this, we evaluated other DTI parameters in the genu in separate, parallel models and found DNAm age residuals to be positively associated with radial diffusivity (RD; $\beta = .18$, $p = .006$) and the apparent diffusion coefficient (ADC; $\beta = .19$, $p = .006$), but not with axial diffusivity (AxD; $\beta = .10$, $p = .13$; see Table 4).

3.4. Accelerated aging and working memory performance via the genu

Given evidence that accelerated aging may manifest in reduced microstructural integrity of the genu, we conducted a follow-up path model to determine if DNAm age residuals were negatively associated with performance on working memory tasks via FA in the genu. FA in the genu has previously been associated with working memory in general (Kennedy and Raz, 2009; Zahr et al., 2009) and concept shifting and problem solving (Zahr et al., 2009) in particular. The Working Memory measurement model (i.e., CFA) fit the data well (Table 1) and all indicators loaded significantly on the latent variable (see Supplementary Materials and Fig. 1). This latent variable was then included in a path model with sex, the two PCs, and WBCs as covariates of DNAm age residuals, and age and sex as covariates of the genu and latent Working Memory. Results showed that FA values in the genu were associated with performance on the Working Memory factor ($\beta = .28$, $p < .001$) and that DNAm age residuals were indirectly and negatively associated with scores on the Working Memory factor via the genu (indirect $\beta = -.05$, $p = .029$; see

Table 2
Unstandardized and standardized direct effects from the models predicting DNAm age residuals.

Predictor	DNAm age residuals (Hannum)		DNAm age residuals (Horvath)	
	Unst. β (SE)	Std. β (SE)	Unst. β (SE)	Std. β (SE)
Sex	−.01 (.01)	−.06 (.06)	−.001 (.01)	−.01 (.06)
PC1	−.04 (.04)	−.06 (.05)	.08[*] (.04)	.12[*] (.05)
PC2	.004 (.04)	.01 (.05)	.03 (.04)	.04 (.06)
CD8T	−.01 (.07)	−.01 (.06)	.05 (.06)	.05 (.06)
CD4T	−.14[**] (.05)	−.16[**] (.06)	−.07 (.05)	−.09 (.06)
NK	.09 (.09)	.07 (.07)	.11 (.09)	.10 (.08)
B cells	−.12 (.10)	−.07 (.06)	−.23[*] (.11)	−.15[*] (.07)
Mono	.20 (.12)	.11 (.07)	.03 (.10)	.02 (.06)
Lifetime PTSD severity	.02[*] (.01)	.13[*] (.06)	.002 (.01)	.02 (.06)

Note: SE = standard error; PC = principal component (for ancestral variation); CD8T = CD8 t-cells; CD4T = CD4 t-cells, NK = natural killer cells, Mono = monocytes; PTSD = posttraumatic stress disorder; Unst. = unstandardized; Std. = standardized, DNAm = DNA methylation.
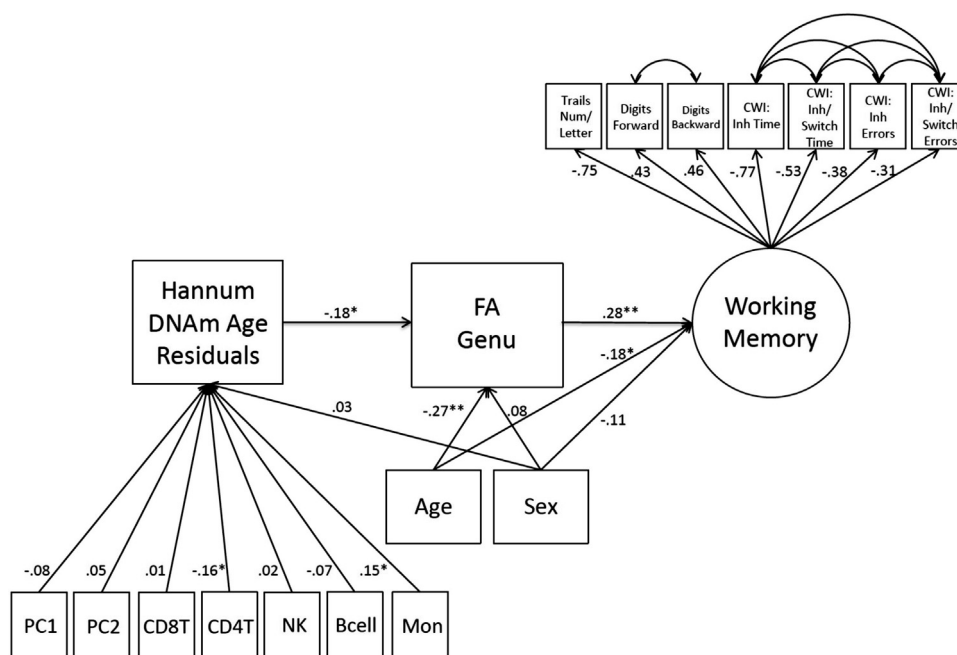
[*] $p < .05$.

[**] $p < .01$.

Fig. 1. The figure shows the path model in which advanced DNAm age residuals were associated with poorer working memory performance via FA in the genu. All paths are fully standardized. The factor loadings on the working memory latent variable were significant at the $p \leq .001$ level. The working memory variable was keyed such that higher scores reflected improved working memory. Correlated residuals among subtests from the same neuropsychological measure were specified, as denoted by curved double headed arrows. DNAm = DNA methylation; PC = principal component; CD8T = CD8 t-cells; CD4T = CD4 t-cells, NK = natural killer cell, Mon = monocytes; FA = fractional anisotropy; Num = number; CWI = Color–Word Interference Test; Inh = inhibition; Switch = switching. $^*p < .05.$ $^{**}p < .001.$

Fig. 1).[3] This model explained 15% of the variance in the Working Memory latent variable.

4. Discussion

Advancing the understanding of mechanisms linking PTSD to pre-mature morbidity and mortality is important given the prevalence of chronic PTSD and the high individual and societal costs associated with it (Bruffaerts et al., 2012). Emerging evidence suggests that PTSD may be associated with accelerated cellular aging and, at least partially through this, linked to various adverse health outcomes (Lohr et al., 2015; Miller and Sadeh, 2014) but, until recently, research on accelerated aging has been limited by the challenges associated with measuring cellular age. The groundbreaking development of DNAm age algorithms that provide reliable biomarkers of chronological age (Hannum et al., 2013; Horvath, 2013) is an opening for achieving new insights into mechanisms of cellular aging in the epigenome and the influence of environmental factors and psychopathology on these processes. In this study, we found that PTSD severity was positively associated with DNAm age residualized for chronological age using Hannum et al.'s (2013) model of methylation age, and that these residuals were negatively associated with neural integrity in the genu of the corpus callosum. DNAm age residuals were also negatively associated with working memory via neural integrity of the genu. These findings are consistent with the hypothesis that PTSD is associated with accelerated cellular aging in DNAm and that accelerated aging in DNAm is related to neuroanatomical and cognitive decline. Findings of this study are also broadly consistent with that of prior studies using telomere length as a metric of aging which indicate that PTSD is associated with shortened telomere length

(Jergović et al., 2014; Lohr et al., 2015; Tyrka et al., 2015; Zhang et al., 2014) and that shortened telomere length is associated with decreased brain volume (King et al., 2014). Our results contrast with those reported by Boks et al. (2015) who found that PTSD predicted decreased Horvath DNAm age, though the comparison is imperfect because Boks et al. did not residualize estimated DNAm age on chronological age.

Our neuroimaging analyses focused on brain ROIs most affected by aging—the frontal cortices and the genu of the corpus callosum. Hannum DNAm age residuals were nominally associated with reduced integrity of the left rostral anterior cingulate cortex and frontal middle gyrus, though neither of these associations survived multiple testing correction; additional research in independent samples is needed to test the replicability of these associations. Results provided stronger support for a link between DNAm age and decreased FA and increased RD and ADC in the genu, a pattern observed previously in association with chronological age (Bennett et al., 2010). These effects are thought to reflect degradation in both the axon fibers and the myelin sheaths around them (Bennett et al., 2010). The genu plays a critical role in communication and coordination of the dorsolateral prefrontal cortices, and as such, underlies working memory performance and executive functions (Kennedy and Raz, 2009; Zahr et al., 2009). Loss of neural integrity in this region has also been linked to neurocognitive disorders, including Alzheimer's disease (Alves et al., 2012; Di Paola et al., 2010). It is thought to be a late myelinating region of the corpus callosum that is composed of long, small diameter, thinly myelinated and easily damaged commissural fibers that transmit information relatively slowly across the hemispheres (Aboitiz et al., 1992; Kochunov et al., 2007, 2012; Pfefferbaum et al., 2000; but see: Stricker et al., 2015).

Premature decline in genu integrity is consistent with the "white matter retrogenesis" model of aging which posits that developmentally late myelinating, typically anterior, fibers are the first to degrade with age and are more sensitive to illness and injury relative to early myelinating and more posterior tracts (Brickman et al., 2012). It is also consistent with theory suggesting that

---

[3] In a separate model, we also included a direct effect of DNAm age residuals in association with the working memory factor and found that this path was not significant ($\beta = .07$, $p = .43$).

Table 3
Estimates for Hannum models predicting left and right hemisphere frontal cortex parcellations.

Dependent variable (L/R)	Predictor					
	DNAm age residuals (Hannum)		Age		Sex	
	Unst. β (SE)	Std. β (SE)	Unst. β (SE)	Std. β (SE)	Unst. β (SE)	Std. β (SE)
Caudal ACC	−.50/−.07 (.43/.09)	−.08/−.04 (.07/.06)	.00/.00 (.002/.001)	−.01/−.01 (.06/.07)	−.04/−.01 (.05/.01)	−.04/−.05 (.06/.06)
Central middle frontal cortex	−.05/.02 (.04/.04)	−.07/.03 (.07/.07)	−.001*/.00 (.00/.00)	−.16*/−.06 (.07/.08)	−.01†/−.004 (.01/.004)	−.12/−.04 (.05/.05)
Lateral orbital frontal cortex	−.02/−.03 (.04/.03)	−.03/−.05 (.07/.06)	−.001***/−.001** (.00/.00)	−.27**/−.34** (.07/.06)	−.01/−.01 (.003/.01)	−.07/−.12 (.04/.06)
Medial orbital frontal cortex	−.05/−.04 (.05/.05)	−.07/−.06 (.07/.06)	.00†/.00 (.00/.00)	−.13†/−.13 (.07/.07)	−.01/−.01 (.01/.01)	−.07/−.06 (.05/.06)
Pars opercularis	−.06/−.05 (.04/.05)	−.09/−.07 (.07/.07)	−.001***/−.001*** (.00/.00)	−.31***/−.30*** (.07/.07)	−.01/−.003 (.004/.01)	−.07/−.10 (.05/.05)
Pars orbitalis	−.02/−.15 (.06/.12)	−.02/−.08 (.06/.06)	−.001‡/−.001 (.00/.001)	−.19†/−.07 (.06/.06)	−.01/−.03 (.01/.02)	−.09/−.10 (.07/.06)
Pars triangularis	.01/−.01 (.04/.05)	.01*/−.02 (.06/.07)	−.001***/−.001 *** (.00/.00)	−.23‡/−.27*** (.07/.06)	−.002/.002 (.01/.01)	−.02/.02 (.05/.06)
Rostral ACC	−.20†/−.09 (.09/.08)	−.13†/−.07 (.06/.07)	−.001*/.00 (.00/.00)	−.12†/−.01 (.06/.07)	−.01/−.02 (.01/.01)	−.03/−.11 (.06/.06)
Rostral middle frontal cortex	−.08*/−.04 (.04/.04)	−.13†/−.06 (.07/.07)	−.001*/−.001*** (.00/.00)	−.23‡/−.28** (.07/.07)	−.01/−.01* (.01/.01)	−.11/−.13* (.06/.06)
Superior frontal gyrus	−.05/−.05 (.04/.04)	−.09/−.08 (.07/.07)	.00*/.00* (.00/.00)	−.16*/−.16* (.07/.08)	−.01*/−.01 (.004/.004)	−.12/−.09 (.05/.05)

Note: the first value presented in each cell is for the left hemisphere and the second value listed is for the right hemisphere. All parcellations are indexed by fractional anisotropy. DNAm = DNA methylation; Unst. = unstandardized; Std. = standardized; ACC = anterior cingulate cortex; SE = standard error.

  * $p < .05$.
  ** $p < .01$.
  *** $p < .001$.
  † $p = .05$.
  ‡ $p = .001$.

myelin sheaths in the genu, and other late myelinating tracts connecting association cortices, have high metabolic requirements in order to preserve and repair myelin sheaths, making these regions susceptible to insults that adversely affect central metabolic processes (Bartzokis, 2004). Epigenetic modifications may contribute to this, given that DNAm partially regulates the process of differentiation into myelin expressing cells (Liu et al., 2010); additional research is needed to evaluate if epigenetic mechanisms underlie potential changes in central nervous system metabolism and myelin production and maintenance. Other factors that may affect central nervous system metabolism include poor cerebral vascular health (Kochunov et al., 2007), glucocorticoids (Bartzokis, 2004), and oxidative stress (Bartzokis, 2004); these systems are also implicated in both PTSD and accelerated aging (Epel et al., 2004; Lohr et al., 2015; Logue et al., 2015; Miller and Sadeh, 2014; Williamson et al., 2015). Metabolic deficiencies put the region at risk for demyelination and neuronal death, which may be evidenced in cognitive decline (Bartzokis, 2004; Lu et al., 2013). The fact that we found effects in the genu in a relatively young sample of veterans raises the possibility that these are the early signs of neurodegeneration. Of course, longitudinal studies are needed to determine if PTSD-related accelerated aging becomes more widespread in the brain with advancing age and if the effects observed here are harbingers for subsequent pathology such as onset of dementing disorders, which have previously been associated with PTSD (Qureshi et al., 2010).

Significant associations with PTSD and neuroimaging parameters were found for the Hannum et al. (2013) but not Horvath (2013) DNAm age algorithm. These models differ in many ways, despite showing similar bivariate relationships to chronological age. For example, the Hannum et al. algorithm was developed on data from whole blood (though validated in other tissues and independent samples) whereas the Horvath model was developed using multiple tissue types. The models have just six overlapping loci and eleven overlapping genes, suggesting that they are fairly distinct from one another, and it is conceivable the methylation loci included in the Hannum model are more sensitive to hematologic conditions of particular relevance to PTSD (e.g., oxidative stress, inflammation, glucocorticoid activation). It is likely that neither model can capture all the pathophysiology that might be implicated in PTSD-related accelerated aging. In the future it may be possible to further adjust the DNAm age algorithms to index more disease-specific forms of accelerated cellular aging.

These conclusions should be tempered against the study limitations, the primary of which was that the data were cross-sectional so causal inferences are limited and longitudinal studies are needed. Given that chronological age is so highly correlated with DNAm age, this leaves little remaining variance in DNAm age estimates, and is likely a reason that effect sizes related to DNAm age residuals were small in magnitude. This is a challenge that all studies focused on accelerated (or decelerated) aging in DNAm will have to address and may require new statistical approaches for modeling epigenetic cellular age as distinct from chronological age. We also did not measure WBCs directly, thus these were estimated using a well validated and commonly employed method (Houseman et al., 2012), though the validity of this method in this specific sample is unknown. In addition, DNAm age was estimated from whole blood and concerns have been raised about the extent to which peripheral DNAm corresponds to DNAm in brain tissue (Tylee et al., 2013). These concerns are tempered in the context of using peripheral DNAm age as a biomarker of accelerated cellular aging, as opposed to an index of a specific brain mechanism. Moreover, Horvath (2013) demonstrated that his DNAm age estimates generalized to brain tissue (though to our knowledge this has not yet been evaluated for the Hannum model) and our results support the relevance of this peripheral marker to neural integrity. Together,

Table 4
Unstandardized and standardized effects from the Hannum models predicting neural integrity of the genu.

Predictor	FA		RD		ADC		AxD	
	Unst. β (SE)	Std. β (SE)	Unst. β (SE)	Std. β (SE)	Unst. β (SE)	Std. β (SE)	Unst. β (SE)	Std. β (SE)
Sex	.01 (.01)	.07 (.05)	−.01 (.01)	−.07 (.06)	−.01 (.01)	−.06 (.06)	−.002 (.02)	−.01 (.07)
Age	−.001[***] (.00)	−.28[***] (.06)	.002[***] (.00)	.23[***] (.06)	.001 (.00)	.10 (.07)	−.001[*] (.001)	−.16[*] (.07)
DNAm age residuals	−.16[*] (.06)	−.17[**] (.07)	.24[**] (.09)	.18[**] (.07)	.22[**] (.08)	.19[**] (.07)	.17 (.11)	.10 (.07)

Note: FA = fractional anisotropy; RD = radial diffusivity; ADC = apparent diffusion coefficient; AxD = axial diffusivity; DNAm = DNA methylation; Unst. = unstandardized; Std. = standardized; SE = standard error.

these findings suggest that peripheral DNAm age estimates could prove to be as proxy for DNAm age in the brain. Finally, it is unclear the extent to which results will generalize to non-veterans, exclusively female samples, older cohorts, or other populations, or if these or other sample characteristics might moderate the observed associations; additional research is required to address these study limitations. Strengths of the study include the large sample size for neuroimaging genetics research, the well-assessed sample with respect to PTSD, the use of chip-based technologies for capturing DNAm and of DTI for capturing neural integrity, and our focus on a promising new index of age in association with both PTSD and neurodegeneration.

In conclusion, findings suggest that PTSD may levy a heavy toll on the body reflected, in part, as accelerated cellular aging in the epigenome. Accelerated aging as evidenced by advanced DNAm age estimates may be manifested in degradation in the neural integrity of microstructural cells in the genu and working memory deficits. This suggests that efforts to prevent PTSD in the acute aftermath of trauma exposure (i.e., secondary prevention; Maccani et al., 2012) have the potential to reduce the likelihood of not just PTSD, but of PTSD-related accelerated aging and adverse health consequences, such as pre-morbid medical conditions and neural and cognitive decline. Findings point to the clinical significance of PTSD-related accelerated aging and to the relevance of peripheral markers of DNAm to brain structure and neurocognitive performance.

Disclosures

Contributions

Authors Wolf, Logue, Hayes, Sadeh, and Miller contributed to the conception and design of the study. Authors Wolf, Logue, Schichman, Stone, Salat, Milberg, McGlinchey, and Miller contributed to the acquisition of data and the interpretation of data. Authors Wolf, Logue, and Miller contributed to the data analyses. All authors contributed to the drafting and/or critical revision of this manuscript for important intellectual content. All authors provided final approval of the submitted manuscript.

Acknowledgements

Appendix A. Supplementary data

Supplementary data associated with this article can be found, in the online version, at http://dx.doi.org/10.1016/j.psyneuen.2015.09.020.

References

Aboitiz, F., Scheibel, A.B., Fisher, R.S., Zaidel, E., 1992. Fiber composition of the human corpus callosum. Brain Res. 598, 143–153.

Alves, G.S., O'Dwyer, L., Jurcoane, A., Oertel-Knöchel, V., Prvulovic, D., Sudo, F., Alves, C.E., Valente, L., Moreira, D., Fußer, F., Karakaya, T., Pantel, J., Engelhardt, E., Laks, J., 2012. Different patterns of white matter degeneration using multiple diffusion indices and volumetric data in mild cognitive impairment and Alzheimer patients. PLoS One 7, e52859.

Aryee, M.J., Jaffe, A.E., Corrada-Bravo, H., Ladd-Acosta, C., Feinberg, A.P., Hansen, K.D., Irizarry, R.A., 2014. Minfi: a flexible and comprehensive bioconductor package for the analysis of Infinium DNA methylation microarrays. Bioinformatics 30, 1363–1369.

Bartzokis, G., 2004. Age-related myelin breakdown: a developmental model of cognitive decline and Alzheimer's disease. Neurobiol. Aging 25, 5–18.

Bennett, I.J., Madden, D.J., Vaidya, C.J., Howard, D.V., Howard Jr., J.H., 2010. Age-related differences in multiple measures of white matter integrity: a diffusion tensor imaging study of healthy aging. Hum. Brain. Mapping 31, 378–390.

Blake, D.D., Weathers, F.W., Nagy, L.M., Kaloupek, D.G., Gusman, F.D., Charney, D.S., Keane, T.M., 1995. The development of a Clinician-Administered PTSD Scale. J. Trauma. Stress 8, 75–90.

Boks, M.P., van Mierlo, H.C., Rutten, B.P., Radstake, T.R., De Witte, L., Geuze, E., Horvath, S., Schalkwyk, L.C., Vinkers, C.H., Broen, J.C., Vermetten, E., 2015. Longitudinal changes of telomere length and epigenetic age related to traumatic stress and post-traumatic stress disorder. Psychoneuroendocrinology 51, 506–512.

Brickman, A.M., Meier, I.B., Korgaonkar, M.S., Provenzano, F.A., Grieve, S.M., Siedlecki, K.L., Wasserman, B.T., Williams, L.M., Zimmerman, M.E., 2012. Testing the white matter retrogenesis hypothesis of cognitive aging. Neurobiol. Aging 33, 1699–1715.

Bruffaerts, R., Vilagut, G., Demyttenaere, K., Alonso, J., Alhamzawi, A., Andrade, L.H., Benjet, C., Bromet, E., Bunting, B., de Girolamo, G., Florescu, S., Gureje, O., Haro, J.M., He, Y., Hinkov, H., Hu, C., Karam, E.G., Lepine, J.P., Levinson, D., Matschinger, H., Nakane, Y., Ormel, J., Posada-Villa, J., Scott, K.M., Varghese, M., Williams, D.R., Xavier, M., Kessler, R.C., 2012. Role of common mental and physical disorders in partial disability around the world. Br. J. Psychiatry 200, 454–461.

Burgmans, S., van Boxtel, M.P., Gronenschild, E.H., Vuurman, E.F., Hofman, P., Uylings, H.B., Jolles, J., Raz, N., 2010. Multiple indicators of age-related differences in cerebral white matter and the modifying effects of hypertension. Neuroimage 49, 2083–2093.

Delis, D.C., Kaplan, E., Kramer, J.H., 2001. D-KEFs Examiners and Technical Manual. Pearson Education, San Antonio, Texas.

Di Paola, M., Spalletta, G., Caltagirone, C., 2010. In vivo structural neuroanatomy of corpus callosum in Alzheimer's disease and mild cognitive impairment using different MRI techniques: a review. J. Alzheimers Dis. 20, 67–95.

Epel, E.S., 2009. Psychological and metabolic stress: a recipe for accelerated aging? Hormones 8, 7–22.

Epel, E.S., Blackburn, E.H., Lin, J., Dhabhar, F.S., Adler, N.E., Morrow, J.D., Cawthon, R.M., 2004. Accelerated telomere shortening in response to life stress. Proc. Natl. Acad. Sci. U. S. A. 101, 17312–17315.

Good, C.D., Johnsrude, I.S., Ashburner, J., Henson, R.N., Friston, K.J., Frackowiak, R.S., 2001. A voxel-based morphometric study of ageing in 465 normal adult human brains. Neuroimage 14, 21–36.

Hannum, G., Guinney, J., Zhao, L., Zhang, L., Hughes, g., Sadda, S., Klotzle, B., Bibikova, M., Fan, J.B., Gao, Y., Deconde, R., Chen, M., Rajapakse, I., Friend, S., Ideker, T., Zhang, K., 2013. Genome-wide methylation profiles reveal quantitative views of human aging rates. Mol. Cell 49, 359–367.

Hofer, S., Frahm, J., 2006. Topography of the human corpus callosum revisited—comprehensive fiber tractography using diffusion tensor magnetic resonance imaging. Neuroimage 32, 989–994.

Horvath, S., 2013. DNA methylation age of human tissues and cell types. Genome Biol. 14, R115.

Horvath, S., Erhart, W., Brosch, M., Ammerpohl, O., von Schönfels, W., Ahrens, M., Heits, N., Bell, J.T., Tsai, P.C., Spector, T.D., Deloukas, P., Siebert, R., Sipos, B., Becker, T., Röcken, C., Schafmayer, C., Hampe, J., 2014. Obesity accelerates epigenetic aging of human liver. Proc. Natl. Acad. Sci. U. S. A. 111, 15538–15543.

Houseman, E.A., Accomando, W.P., Koestler, D.C., Christensen, B.C., Marsit, C.J., Nelson, H.H., Wiencke, J.K., Kelsey, K.T., 2012. DNA methylation arrays as surrogate measures of cell mixture distribution. BMC Bioinf. 13, 86.

Hu, L.T., Bentler, P.M., 1999. Cutoff criteria for fit indexes in covariance structure analysis: conventional criteria versus new alternatives. Struct. Equ. Model. 6, 1–55.

Jaffe, A.E., Irizarry, R.A., 2014. Accounting for cellular heterogeneity is critical in epigenome-wide association studies. Genome Biol. 15, R31.

Jergović, M., Tomičević, M., Vidović, A., Bendelja, K., Savić, A., Vojvoda, V., Rac, D., Lovrić-Čavar, D., Rabatić, S., Jovanovic, T., Sabioncello, A., 2014. Telomere shortening and immune activity in war veterans with posttraumatic stress disorder. Prog. Neuropsychopharmacol. Biol. Psychiatry 54, 275–283.

Kennedy, K.M., Raz, N., 2009. Aging white matter and cognition: differential effects of regional variations in diffusion properties on memory, executive functions, and speed. Neuropsychologia 47, 916–927.

King, K.S., Kozlitina, J., Rosenberg, R.N., Peshock, R.M., McColl, R.W., Garcia, C.K., 2014. Effect of leukocyte telomere length on total and regional brain volumes in a large population-based cohort. JAMA Neurol. 71, 1247–1254.

Kochunov, P., Thompson, P.M., Lancaster, J.L., Bartzokis, G., Smith, S., Coyle, T., Royall, D.R., Laird, A., Fox, P.T., 2007. Relationship between white matter fractional anisotropy and other indices of cerebral health in normal aging: tract-based spatial statistics study of aging. Neuroimage 35, 478–487.

Kochunov, P., Williamson, D.E., Lancaster, J., Fox, P., Cornell, J., Blangero, J., Glahn, D.C., 2012. Fractional anisotropy of water diffusion in cerebral white matter across the lifespan. Neurobiol. Aging 33, 9–20.

Lindqvist, D., Epel, E.S., Mellon, S.H., Penninx, B.W., Révész, D., Verhoeven, J.E., Reus, V.I., Lin, J., Mahan, L., Hough, C.M., Rosser, R., Bersani, F.S., Blackburn, E.H., Wolkowitz, O.M., 2015. Psychiatric disorders and leukocyte telomere length: underlying mechanisms linking mental illness with cellular aging. Neurosci. Biobehav. Rev. 55, 333–364.

Liu, J., Sandoval, J., Doh, S.T., Cai, L., López-Rodas, G., Casaccia, P., 2010. Epigenetic modifiers are necessary but not sufficient for reprogramming non-myelinating cells into myelin gene-expressing cells. PLoS One 5, e13023.

Logue, M.W., Smith, A.K., Baldwin, C., Wolf, E.J., Guffanti, G., Melista, E., Ratanatharathorn, A., Stone, A., Schichman, S., Humphries, D., Binder, E.B., Arloth, J., Menke, A., Uddin, M., Wildman, D., Galea, S., Aiello, A.E., Koenen, K.C., Miller, M.W., 2015. A transcriptome-wide analysis of gene expression in PTSD implicates genes involved in the glucocorticoid receptor network and neural responses to stress. Psychoneuroendocrinology 57, 1–13.

Lohr, J.B., Palmer, B.W., Eidt, C.A., Aailaboyina, S., Mausbach, B., Wolkowitz, O.M., Thorp, S.R., Jeste, D.V., 2015. Is post-traumatic stress disorder associated with premature senescence? A review of the literature. Am. J. Geriatr. Psychiatry 23, 709–725.

Lu, P.H., Lee, G.J., Tishler, T.A., Meghpara, M., Thompson, P.M., Bartzokis, G., 2013. Myelin breakdown mediates age-related slowing in cognitive processing speed in healthy elderly men. Brain Cogn. 81, 131–138.

Maccani, M.A., Delahanty, D.L., Nugent, N.R., Berkowitz, S.J., 2012. Pharmacological secondary prevention of PTSD in youth: challenges and opportunities for advancement. J. Trauma. Stress 25, 543–550.

Marioni, R.E., Shah, S., McRae, A.F., Chen, B.H., Colicino, E., Harris, S.E., Gibson, J., Henders, A.K., Redmond, P., Cox, S.R., Pattie, A., Corley, J., Murphy, L., Martin, N.G., Montogomery, G.W., Feinberg, A.P., Fallin, M.D., Multhaup, M.L., Jaffe, A.E., Joehanes, R., Schwartz, J., Just, A.C., Lunetta, K.L., Murabito, J.M., Starr, J.M., Horvath, S., Baccarelli, A.A., Levy, D., Visscher, P.M., Wray, N.R., Dreary, I.J., 2015a. DNA methylation age of blood predicts all-cause mortality in later life. Genome Biol. 16, 25.

Marioni, R.E., Shah, S., McRae, A.F., Ritchie, S.J., Muniz-Terrera, G., Harris, S.E., Gibson, J., Redmond, P., Cox, S.R., Pattie, A., Corley, J., Taylor, A., Murphy, L., Starr, J.M., Horvath, S., Visscher, P.M., Wray, N.R., Deary, I.J., 2015b. The

epigenetic clock is correlated with physical and cognitive fitness in the Lothian Birth Cohort 1936. Int. J. Epidemiol., http://dx.doi.org/10.1093/ije/dyu277, epub ahead of print.

Miller, M.W., Sadeh, N., 2014. Traumatic stress, oxidative stress and post-traumatic stress disorder: neurodegeneration and the accelerated-aging hypothesis. Mol. Psychiatry 19, 1156–1162.

Moreno-Villanueva, M., Morath, J., Vanhooren, V., Elbert, T., Kolassa, S., Libert, C., Bürkle, A., Kolassa, I.T., 2013. N-Glycosylation profiling of plasma provides evidence for accelerated physiological aging in post-traumatic stress disorder. Transl. Psychiatry 3, e320.

Muthén, L.K., Muthén, B.O., 2012. Mplus User's Guide. Muthén & Muthén, Los Angeles, California.

Park, D.C., Lautenschlager, G., Hedden, T., Davidson, N.S., Smith, A.D., Smith, P.K., 2002. Models of visuospatial and verbal memory across the adult life span. Psychol. Aging 17, 299–320.

Pfefferbaum, A., Sullivan, E.V., Hedehus, M., Lim, K.O., Adalsteinsson, E., Moseley, M., 2000. Age-related decline in brain white matter anisotropy measured with spatially corrected echo-planar diffusion tensor imaging. Magn. Reson. Med. 44, 259–268.

Qureshi, S.U., Kimbrell, T., Pyne, J.M., Magruder, K.M., Hudson, T.J., Petersen, N.J., Yu, H.J., Schulz, P.E., Kunik, M.E., 2010. Greater prevalence and incidence of dementia in older veterans with posttraumatic stress disorder. J. Am. Geriatr. Soc. 58, 1627–1633.

Resnick, S.M., Pham, D.L., Kraut, M.A., Zonderman, A.B., Davatzikos, C., 2003. Longitudinal magnetic resonance imaging studies of older adults: a shrinking brain. J. Neurosci. 23, 3295–3301.

Salat, D.H., Buckner, R.L., Snyder, A.Z., Greve, D.N., Desikan, R.S., Busa, E., Morris, J.C., Dale, A.M., Fischl, B., 2004. Thinning of the cerebral cortex in aging. Cereb. Cortex 14, 721–730.

Salat, D.H., Tuch, D.S., Greve, D.N., van der Kouwe, A.J., Hevelone, N.D., Zaleta, A.K., Rosen, B.R., Fischl, B., Corkin, S., Rosas, H.D., Dale, A.M., 2005a. Age-related alterations in white matter microstructure measured by diffusion tensor imaging. Neurobiol. Aging 26, 1215–1227.

Salat, D.H., Tuch, D.S., Hevelone, N.D., Fischl, B., Corkin, S., Rosas, H.D., Dale, A.M., 2005b. Age-related changes in prefrontal white matter measured by diffusion tensor imaging. Ann. N. Y. Acad. Sci. 1064, 37–49.

Stricker, N.H., Salat, D.H., Kuhn, T.P., Foley, J.M., Price, J.S., Westlye, L.T., Esterman, M.S., McGlinchey, R.E., Milberg, W.P., Leritz, E.C., 2015. Mild cognitive impairment is associated with white matter integrity changes in late-myelinating regions within the corpus callosum. Am. J. Alzheimers Dis. Other Demen., http://dx.doi.org/10.1177/1533317515578257, epub ahead of print.

Teschendorff, A.E., Marabita, F., Lechner, M., Bartlett, T., Tegner, J., Gomez-Cabrero, D., Beck, S., 2013. A beta-mixture quantile normalization method for correcting probe design bias in Illumina Infinium 450k DNA methylation data. Bioinformatics 29, 189–196.

Tylee, D.S., Kawaguchi, D.M., Glatt, S.J., 2013. On the outside, looking in: a review and evaluation of the comparability of blood and brain -omes. Am. J. Med. Genet. B Neuropsychiatr. Genet. 162B, 595–603.

Tyrka, A.R., Parade, S.H., Price, L.H., Kao, H.T., Porton, B., Philip, N.S., Welch, E.S., Carpenter, L.L., 2015. Alterations of mitochondrial DNA copy number and telomere length with early adversity and psychopathology. Biol. Psychiatry, http://dx.doi.org/10.1016/j.biopsych.2014.12.025, epub ahead of print.

Voineskos, A.N., Rajji, T.K., Lobaugh, N.J., Miranda, D., Shenton, M.E., Kennedy, J.L., Pollock, B.G., Mulsant, B.H., 2012. Age-related decline in white matter tract integrity and cognitive performance: a DTI tractography and structural equation modeling study. Neurobiol. Aging 33, 21–34.

Weathers, F.W., Ruscio, A.M., Keane, T.M., 1999. Psychometric properties of nine scoring rules for the Clinician-Administered Posttraumatic Stress Disorder Scale. Psychol. Assess. 11, 124–133.

Wechsler, D., 1997. Manual for the Wechsler Adult Intelligence Scale-III. Psychological Corporation, San Antonio, Texas.

Williamson, J.B., Porges, E.C., Lamb, D.G., Porges, S.W., 2015. Maladaptive autonomic regulation in PTSD accelerates physiological aging. Front. Psychol. 5, 1571.

Zahr, N.M., Rohlfing, T., Pfefferbaum, A., Sullivan, E.V., 2009. Problem solving, working memory, and motor correlates of association and commissural fiber bundles in normal aging: a quantitative fiber tracking study. Neuroimage 44, 1050–1062.

Zhang, L., Hu, X.Z., Benedek, D.M., Fullerton, C.S., Forsten, R.D., Naifeh, J.A., Li, X., Li, H., Benevides, K.N., Smerin, S., Le, T., Choi, K., Ursano, R.J., 2014. The interaction between stressful life events and leukocyte telomere length is associated with PTSD. Mol. Psychiatry 19, 855–856.